NeuroImage **10,** 114–124 (1999)
Article ID nimg.1999.0449, available online at http://www.idealibrary.com on IDEAL®

Human Brain Activity Related to the Perception of Spatial Features of Objects

Isabelle Faillenot,*,† Jean Decety,*,†,[1] and Marc Jeannerod‡

**INSERM U280, 151 cours Albert Thomas, 69003 Lyon, France; †CERMEP, 59 boulevard Pinel, 69003 Lyon, France; and ‡Institut des Sciences Cognitives, 67 boulevard Pinel, 69675 Bron, France*

Received September 23, 1998

The role of the parietal cortex in visuospatial analysis of object was investigated by cerebral blood flow measurements in seven subjects using positron emission tomography. Data were acquired while subjects performed a matching task requiring the discrimination of simultaneously presented objects based on one of their spatial properties. Three properties were studied separately during three scanning conditions repeated twice: surface orientation, principal axis orientation, and size. Scans were also obtained during a sensorimotor control task (similar visual stimulation, same motor action, voluntary saccades toward each object) as well as during rest (no stimulation, eyes closed). Compared to rest, the three property matching tasks showed the same pattern of activation: the whole occipital lobe, the right intraparietal sulcus (IPS), and the right occipitotemporal (OT) junction. Compared to the control condition, only right IPS and OT junction were significantly activated during discrimination of the spatial properties. The IPS focus was located between the superior parietal lobule and the angular gyrus, and the OT activation overlapped the posterior part of the inferior temporal gyrus and the middle occipital gyrus. These results indicate that discrimination of spatial attributes requires the activation of both the parietal and the temporal cortices of the right hemisphere and provide further evidence that the IPS plays a critical role in visuospatial analysis of objects. © 1999 Academic Press

Key Words: **PET; functional anatomy; vision; perception; object orientation; object size; temporal cortex; parietal cortex**

INTRODUCTION

A well-known model has postulated that the visual cortex is organized into two distinct pathways both originating in the primary visual cortex. The ventral pathway, which reaches the inferotemporal cortex, is involved in object perception whereas the dorsal pathway, which projects into the parietal cortex, is engaged in visuospatial perception (e.g., Ungerleider and Mishkin, 1982). Later, Milner and Goodale substantially reinterpreted these functions on the basis of neuropsychological dissociations. They postulated that both pathways process the same visual information about objects but with different purposes. The dorsal stream would process visual information for controlling actions on objects, whereas the ventral stream would extract cues for object perception and identification (Goodale and Milner, 1992; Milner and Goodale, 1995). Although these two models may provide useful generalizations, they do not fully reflect the complexity of the cortical operations and the close cooperation that exists between both systems (see, for example, Merigan and Maunsell, 1993).

In a previous PET study in human subjects, Faillenot *et al.* (1997b) found that grasping objects involved only parietal regions while shape matching was associated with temporal and parietal activations. The fact that a common parietal region (anterior intraparietal sulcus, IPS) was involved in both tasks underlines that perception and action are not completely independent processes and further demonstrates that the parietal cortex participates in object perception. One possible interpretation of Faillenot *et al.*'s data is that this IPS region plays a role in integrating some spatial properties of objects such as orientation, size, and the relative location of object parts. Those properties are equally important for grasping and for identifying object shape.

This interpretation is congruent with the finding that monkey IPS neurons may exhibit selectivity for 3D structure of objects; e.g., they may fire when an object of the preferred configuration is seen or grasped (for a recent review, see Sakata *et al.*, 1997). In the anterior part of IPS (area AIP), neurons may encode spatial characteristics of objects for manipulation (Taira *et al.*, 1990). In the caudal part of the lateral bank of IPS,

[1] To whom correspondence should be addressed. E-mail: decety@lyon151.inserm.fr.

1053-8119/99 $30.00

neurons may be sensitive to orientation of the longitudinal axes and flat surfaces in 3D space (Ohtsuka *et al.*, 1995; Shikata *et al.*, 1996). Most of them were binocular visual neurons. Furthermore, lesions of the inferior parietal cortex (including the lateral bank of the IPS) impair the discrimination of pattern orientation (Eacott and Gaffan, 1991).

The present study used positron emission tomography (PET) in healthy human subjects to investigate the role of parietal cortex in the perception of visuospatial properties of objects. Three spatial attributes were selected: principal axis orientation (2D), surface orientation (3D), and size of flat objects. These properties are of critical importance for the visuomotor transformation (e.g., for grasping objects, as demonstrated by several psychophysical studies: Desmurget *et al.*, 1995; Paulignan *et al.*, 1997), as well as for recognizing these objects (e.g., Marr, 1982; Biederman, 1987; Kosslyn, 1994). The task chosen was a simultaneous discrimination task. A sensorimotor control and a rest condition were also performed.

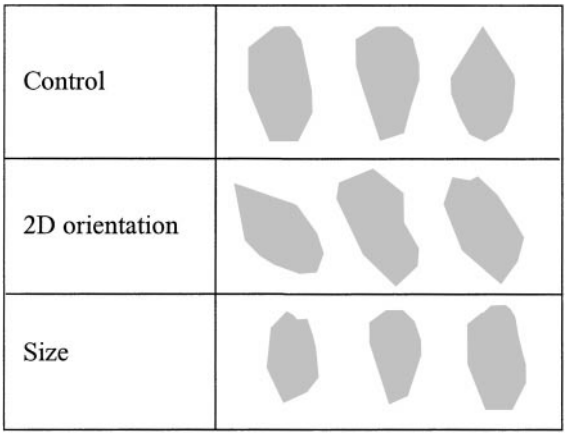

FIG. 1. Examples of stimulation according to each condition. During the control condition, objects were presented vertically, within the frontoparallel plane and their size never changed. For the 2D orientation condition, objects of the same size were within the frontoparallel plane but the principal axis orientation changed. During the size condition, only the object global size changed. 20 shapes with 9 sides were designed. Objects were flat.

MATERIALS AND METHODS

Subjects

Seven right-handed, healthy male volunteers (age 25 ± 1.5 years) participated. They had a normal or corrected-to-normal vision and none had difficulty with stereoscopic vision according to the TNO test (1972). All subjects gave their informed consent and were paid for their participation. This study was approved by the local ethical committee.

Experimental Procedure

Subjects were scanned during three different test tasks, 1 control condition, and 1 resting condition. Each condition was repeated twice. The order of the 10 conditions was randomized across subjects.

During test tasks, only one of the following spatial attributes varied: 2D orientation, 3D orientation, or size. These tasks consisted in comparing one spatial attribute of three objects presented simultaneously. Presentation of stimuli was identical in the three conditions: objects were horizontally aligned at the same virtual distance (Fig. 1). A reference object was positioned in the center of the screen and the two target objects on each side. Within each trial, the three objects had different shapes. By means of a mouse button, and according to the instructions, the subject indicated which one of these objects had the same attribute of interest as the reference object. Three seconds were given to respond before objects disappeared. Then, another trial started after a 0.5-s interval. Before the experiment, the subject performed a short training (about 5 min for each condition) using a different set of stimuli to that used during scanning conditions.

During the 2D orientation condition, objects were presented within the frontoparallel plane. Their principal axis was rotated by an angle of ±10°, ±20°, or ±30° from the vertical axis. Within each trial, the difference in orientation between the reference object and the different target object was 10°, 20°, or 30°. Subjects were instructed to press the button (right or left) indicating which object (right or left) was presented with the same axis orientation as the reference object.

For the 3D orientation condition, objects were presented in a plane rotated around the horizontal and/or vertical axis with an angle of ±30° or ±45°. The angle D between two different planes has been calculated with the formula

$$\cos D = \frac{(\sin x \sin x' + \sin y \sin y' + \cos x \cos x' \cos y \cos y')}{(\sin x^2 + \sin y^2 + \cos x^2 \cos y^2)^{1/2} \cdot (\sin x'^2 + \sin y'^2 + \cos x'^2 \cos y'^2)^{1/2}}$$

where x is the rotation angle around the horizontal axis of the reference plane, y is the rotation angle around the vertical axis of the reference plane, x' is the rotation angle around the horizontal axis of the test plane, and y' is the rotation angle around the vertical axis of the test plane.

Within one trial, the angle D between the two objects presented in different planes ranged from 15° to 110°. Subjects were requested to indicate which one of the two target objects (right or left) was presented in a plane parallel to that of the reference object.

During the size condition, object size ranged from 75 to 125% of the standard object size used in the other conditions. Between two target objects of one trial, size difference was between 8 and 24%. Subjects were

requested to indicate which object (right or left) had the same size as the reference object.

The control condition consisted in a simple visual task that allowed us to record the cerebral perfusion related to object vision and to eye and finger movements. Stimuli presentation was the same as during the test conditions but spatial attributes never changed. Subjects were requested to look at the objects one by one and then to press the right or left mouse button alternatively.

During the rest condition subjects were asked to think nothing in particular and to close their eyes. The visual display was switched off.

Stimuli were presented in a virtual environment system (Provision, UK) which consisted of a helmet connected to a virtual reality transputer-based parallel calculator (Division Ltd. Bristol, UK) in which a 3D stereo image generator was included. The helmet contained two LCD color video screens. Subjects' performances and reaction times were collected by a personal computer connected to the virtual reality system. Only binocular disparity was available for the subjects to perceive the third dimension: shadow, shading, thickness, knowledge of shape, and background reference did not exist in these stimuli. Objects were presented against a nonhomogeneous colored background in order to enhance binocular disparity cues.

Data Acquisition

Brain activity was monitored as relative changes in local cerebral blood flow (rCBF). rCBF was estimated by recording the distribution of radioactivity following injection of $H_2{}^{15}O$. Head movements were restricted with a molded-foam head holder. A transmission scan was obtained using rotating pin sources filled with ^{68}Ge (9 mCi/pin), followed by 10 emission scans 60 s long, separated by 10 min. Stimulation and intravenous bolus injection of 9 mCi started at the same time. The emission scan started automatically when radioactivity reached the brain, about 20 s after the injection time. The PET data were obtained using a Siemens CTI HR+ tomograph with septa retracted operating in high-sensitivity three-dimensional mode. The system has 32 rings which allow us to obtain 63 slices spaced 2.42 mm apart.

Images Analysis

Possible head movements between scans were corrected by aligning all scans on the first one, using automated image registration software (Woods *et al.*, 1993). Then, all images were transformed into a standard space (Talairach and Tournoux, 1988) using a stereotactic normalization (SPM96). This normalizing spatial transformation matches each scan to a template image that already conforms to the standard space. Subsequently, the images were filtered with a low-pass Gaussian filter (FWHM of 12 mm) for smoothing the data. The estimated resolution of the data after smoothing (FWHM) was $14 \times 16 \times 15$ mm.

Statistical analysis was performed using the SPM96 package. In this study, the resulting foci were then characterized in terms of peak height (Z_{max}) and spatial extent (k). The significance of each region is based on the $P\{k, Z\}$ corresponding to the probability of obtaining a region of k, or more, voxels with a peak value Z, at a specified threshold u, in the volume analyzed. The thresholds used in this study were $u = 3.09$ and $k = 255$ (2 cm^3). Stimulus-induced changes in rCBF were considered to be significant when $P\{k, Z\} < 0.05$ after applying a correction for multiple comparisons (Poline and Worsley, 1997). Previous SPM versions used the $P\{Z\}$ the probability that the observed peak height could have occurred by chance over the entire volume. Each peak of a significant region was described in terms of Z score, $P\{Z\}$ corrected, and Talairach coordinates. The corresponding anatomical region was obtained by superimposing significant rCBF changes on a normalized MRI (available in the SPM software) which outlines correspond to those of the averaged normalized PET data.

Some weak activations (i.e., nonsignificant foci with $u > 3.09$, $k > 100$ (0.8 cm^3), and $0.05 < P\{k, Z\} < 0.5$) were considered when additional evidence for their relevance was available either from other studies or from other subtractions from the present study.

Planned Subtractions

Comparison of the control task to rest should show activity related with object vision and with eyes and fingers movements (Control − Rest). Comparison of test tasks to rest should show the same activations in addition to the foci related to spatial attributes analysis and perception (Tests − Rest, where Tests = 3D orientation + 2D orientation + Size). Comparison of test tasks to control should show the structures involved in spatial attributes analysis and perception (Tests − Control). Each test task was compared to the control (3D orientation − Control; 2D orientation − Control; Size − Control) to reveal the specificity of each task. In the three test tasks, only the spatial feature analyzed differed. Thus, the subtractions between these conditions should show the structures specifically involved in the analysis of each attribute tested (3D orientation − 2D orientation; 3D orientation − Size; 2D orientation − Size; 2D orientation − 3D orientation; Size − 3D orientation; Size − 2D orientation). Deactivations were determined by subtracting images acquired during control and test conditions from images acquired during rest conditions (Rest − Control; Rest − Tests).

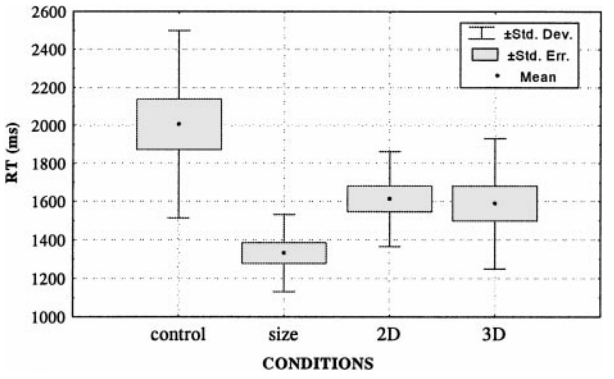

FIG. 2. Group reaction times plot by conditions. The time scaled on the vertical axis does not represent the real RT. Indeed, it includes a constant but unknown amount of time due to stimulation system.

RESULTS

Psychophysical Performance during Scanning (Fig. 2)

Subjects correctly performed the tasks (91.8% correct responses) with best performance for the control (95.8%) and the size (94.4%) conditions and worst performance for the 3D (88.2%) and the 2D (89.4%) orientation tasks. Statistical analysis (ANOVA) on the subjects' reaction times indicated that there was an effect of the conditions ($P < 0.0001$). Post hoc analysis (Scheffe) showed that:

—The 2D and 3D orientation tasks were performed in the same way by subjects ($P = 0.85$).

—The control task was performed slower than other tasks ($P < 0.0001$).

—The size task was performed faster ($P < 0.0001$).

One should note that the "reaction time" of the control condition in fact did not measure a *reaction* time since the subjects were requested to look at objects one by one and then to press a button. In addition, they were not asked to perform the task as quickly as possible.

Control − Rest Subtraction (Table 1, Fig. 3)

When the control condition was compared to the rest condition, two significant foci of rCBF increases appeared. The stronger ($Z_{max} = 7.6$) and wider (126 cm^3) focus covered the entire occipital lobe. Two peaks in this focus were located in the cerebellum, just below the occipital cortex. The second focus was in the left hemisphere, around the central and precentral sulci, where S1, M1, and premotor cortex are located. A weak rCBF increase was observed in the medial frontal gyrus corresponding to the posterior part of the supplementary motor area (SMA proper). Even it did not reach significance, SMA activation is not a surprising finding during a motor task (for a review see Picard and Strick, 1996).

Tests − Rest Subtraction (Table 2)

When the test conditions were compared to the rest condition, the regions found in the previous subtraction were again activated, except for the SMA. rCBF in-

TABLE 1

Subtraction Control − Rest

Anatomical region	BA	Coordinates (mm) x	y	z	Z score	P{Z}	k	P{k, Z}
L calcarine sulcus	17	−4	−78	−8	7.58	<0.001	15785	<0.001
R lingual gyrus	18/17	6	−78	−2	7.24	<0.001		
R cerebellum		24	−48	−18	6.94	<0.001		
R cuneus	18/19	18	−86	18	6.65	<0.001		
L posterior lingual	18	−6	−94	−4	6.62	<0.001		
R posterior lingual	18	4	−92	−2	6.54	<0.001		
R calcarine sulcus	17	16	−92	8	6.52	<0.001		
L middle occipital gyrus	18	−24	−90	2	6.44	<0.001		
L calcarine sulcus	17	−14	−92	12	6.42	<0.001		
L middle occipital gyrus	19	−24	−84	20	6.20	<0.001		
R inferior occipital gyrus	18	28	−90	−4	6.08	<0.001		
L middle occipital gyrus	19	−36	−82	6	4.90	0.009		
L cerebellum		−20	−68	−18	4.57	0.04		
L central sulcus	4/3	−40	−26	54	5.30	0.001	796	0.004
L precentral gyrus	6	−46	0	44	4.25	0.12		
L precentral sulcus	6	−28	−16	64	3.77	0.51		
Medial frontal gyrus	6	12	−2	66	4.48	0.05	343	NS 0.06

Note. Location according to MRI inspection, Brodmann area (BA), Talairach coordinates, *Z* score, and *P*{*Z*} are given for all the peaks of significant foci. Voxel number (*k*) and the significance (*P*{*k*, *Z*}) of each focus are given. L, left; R, right; NS, not significant.

TABLE 2

Subtraction Tests − Rest

	Anatomical region	BA	Coordinates (mm) x	y	z	Z score	P[Z]	k	P[k, Z]
R	calcarine or lingual	17/18	8	−78	−2	7.96	<0.001	21855	<0.001
R	cuneus	18/19	20	−88	18	7.95	<0.001		
L	lingual gyrus	18	−6	−78	−8	7.95	<0.001		
L	calcarine sulcus	17	−10	−94	−6	7.51	<0.001		
L	middle occipital gyrus	18/19	−26	−90	2	7.37	<0.001		
R	inferior occipital gyrus	18/19	28	−90	−4	7.29	<0.001		
R	cerebellum		24	−48	−18	7.10	<0.001		
L	middle occipital gyrus	19	−24	−84	20	7.05	<0.001		
L	inferior occipital gyrus	19	−40	−76	−4	7.04	<0.001		
L	middle occipital gyrus	19	−36	−82	6	6.96	<0.001		
R	intraparietal sulcus	7	24	−66	56	6.61	<0.001		
L	cerebellum		−20	−70	−18	5.95	<0.001		
R	cerebellum (vermis)		12	−56	−16	5.37	0.001		
R	intraparietal sulcus or IPL	40	46	−44	48	4.50	0.05		
R	temporal fusiform gyrus	20	38	−32	−22	3.40	0.89		
L	central sulcus	4/3	−40	−28	56	5.95	<0.001	766	0.001

Note. BA, Brodmann area; L, left; R, right. For details see legend to Table 1.

creased in the whole occipital lobes and in the cortex around the left central sulcus. Moreover, the former focus was not limited to the occipital lobes: it spread into the parietal and temporal lobes. The peak in the parietal cortex was located in or near the IPS and the peak in the temporal cortex was located in the fusiform gyrus. Each test condition compared to the rest condition showed similar results (but *Z* scores were lower in those two latter areas, see Fig. 4).

Tests − Control Subtraction (Table 3, Fig. 5)

Spatial attribute discrimination, compared to the control task, activated two regions in the right hemisphere. One focus was located in the parietal cortex near the intraparietal sulcus between the superior parietal lobule (BA 7) and the angular gyrus (BA 39). The other focus was at the occipitotemporal (OT) junction: it had one peak in the posterior part of the inferior temporal gyrus (ITG) and another peak in the middle occipital gyrus.

3D Orientation, 2D Orientation, and Size versus Control Subtractions (Table 4)

Compared to control, the 3D orientation condition revealed two significant rCBF increases in the right hemisphere. One focus was located in the IPS, and the other in the occipitotemporal junction (BA 19 and 37) extending into the angular gyrus (BA 39). During the 2D orientation and the size conditions, none of the rCBF increases reached the significance level. In order to assess whether IPS and OT junction were involved only during the 3D task or during the three tasks, we looked for these foci among the weak activations. Actually, the size and the 2D conditions compared to the control condition showed only two weak activations: one in the right IPS and another in the OT junction.

Between Test Conditions Subtractions

None of the six subtractions performed between the three test conditions showed a significant rCBF in-

TABLE 3

Subtraction Tests − Control

	Anatomical region	BA	Coordinates (mm) x	y	z	Z score	P[Z]	k	P[k, Z]
R	intraparietal sulcus	7/39	20	−68	50	4.99	0.006	445	0.01
R	inferior temporal gyrus	37	50	−56	−10	4.68	0.02	719	0.006
R	middle occipital gyrus	19	42	−74	−4	4.68	0.02		

Note. BA, Brodmann area; L, left; R, right. For details see legend to Table 1.

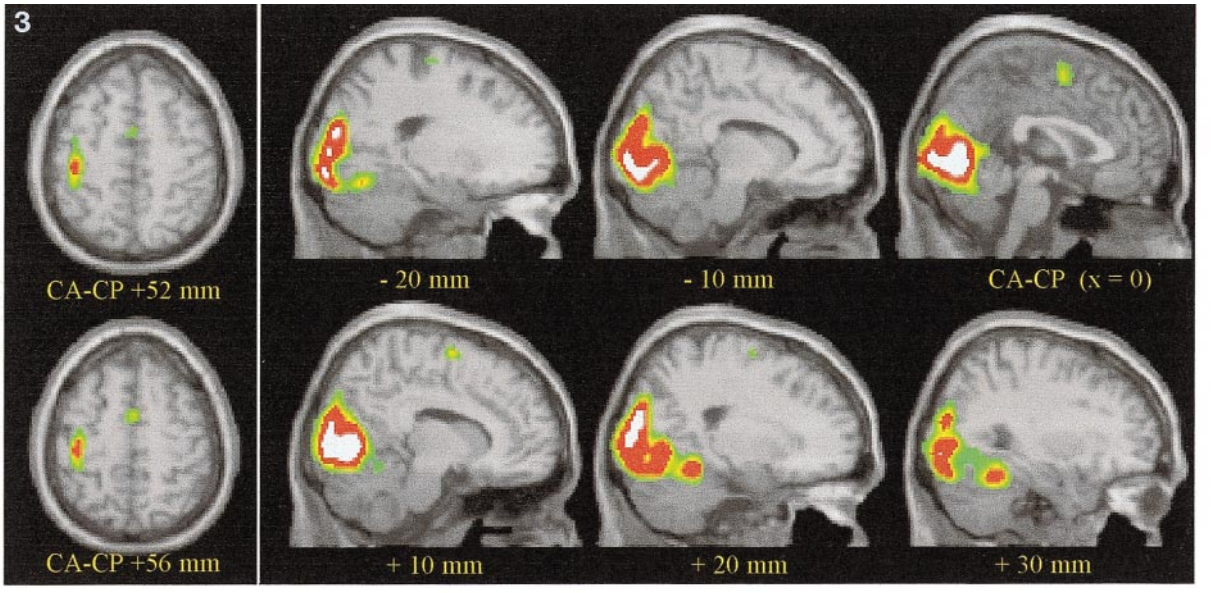

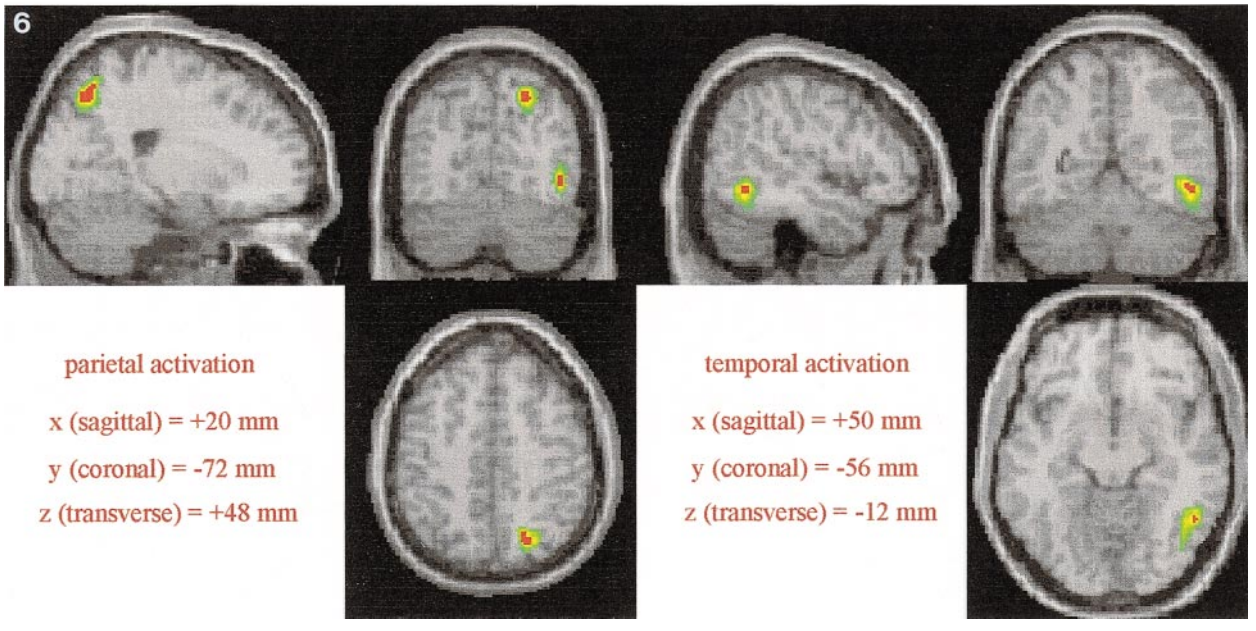

FIG. 3. Cerebral regions activated during the control condition versus Rest, superimposed on sections of a normalized MRI (see Table 1). (Left) Transverse sections showing sensorimotor activations (S1, M1, and SMA). (Right) Sagittal sections showing occipital activations. Numbers bellow the slices indicate the distance (in mm) from the midline (*x* coordinate). Green to yellow, pixels with *Z* score between 3.1 and 4.5 (0.99 > corrected $P\{Z\}$ value > 0.05). Red, *Z* score between 4.5 and 5.5 (0.05 > $P\{Z\}$ > 0.0001). White, *Z* score greater than 5.5.

FIG. 4. rCBF increases during each test Condition versus Rest superimposed on a same coronal MRI slice. Each image has its own color scale but only voxels with *Z* score > 3.1 are colored.

FIG. 6. Significant rCBF increases during the test conditions compared with the control condition, superimposed on a normalized MRI (see Table 3). (Left) Orthogonal sections showing the parietal activation. (Right) Orthogonal sections showing the temporal activation. Numbers indicate the distance of each section from the anterior commissure position. Green to yellow, pixels with *Z* score between 3.1 and 4.5 (0.99 > corrected $P\{Z\}$ value > 0.05). Red, *Z* score greater than 4.5 ($P\{Z\} < 0.05$).

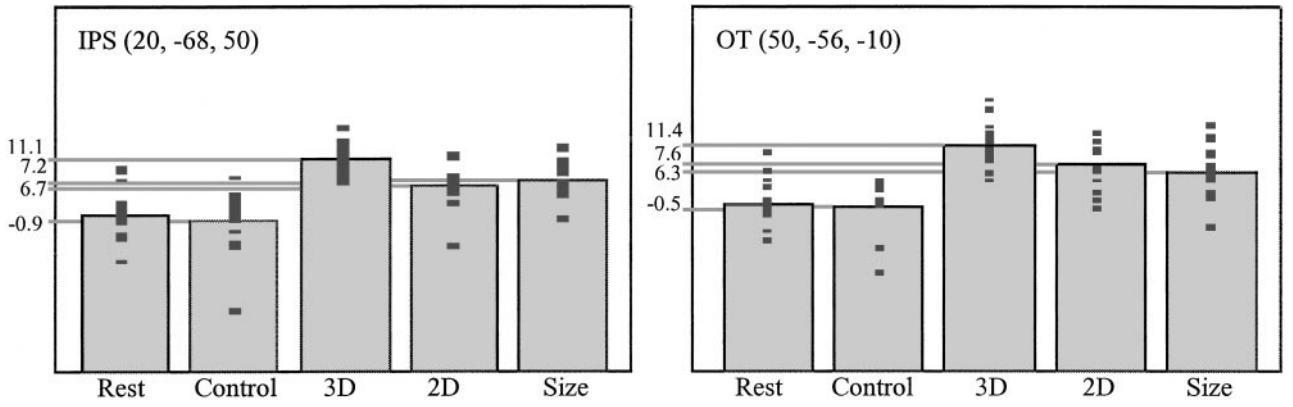

FIG. 5. Activity profiles of the local maximum of the two main foci: IPS and OT junction. Adjusted response is plotted for the five different conditions. Dark dots represent the activity of this voxel for each scan acquired during this condition (two dots per subject and per condition). The figures on the *Y* axis represent the percentage of variation compared to the mean adjusted response during rest.

crease. Neither IPS nor the OT junction was present among the weak activations.

Deactivations (Table 5)

Deactivations were numerous and widely distributed. The main deactivation spread over the right superior temporal gyrus and into the superior temporal sulcus. During the test conditions, the superior part of the left temporal lobe was also deactivated. In addition, rCBF decreased in the posterior cingular cortex during the test conditions. The Rest − Control subtraction yielded two more foci, the anatomical location of which remained undetermined because they were between two lobes or between two different structures.

The main rCBF reductions are located in auditory cortex, as already shown during similar visual tasks (Haxby *et al.*, 1994; Courtney *et al.*, 1996; Shulman *et al.*, 1997). As suggested by Haxby *et al.* (1994), selective attention to visual stimuli may be associated with suppression of neural activity in areas that process input from unattended sensory modalities. This idea is coherent with the present observation that there is a relation between the task difficulty and the extent of the deactivation. Indeed, only 14.9 cm^3 were significantly deactivated during the control condition whereas 80.5 cm^3 were deactivated during the test conditions. Moreover, the size condition which was easier than the orientation conditions shows only 15.1 cm^3 deactivated, whereas the 2D and 3D orientation conditions show about 92 cm^3 deactivated. This relation between the size of the deactivation and the level of difficulty was previously observed during an experiment on motor learning (Jenkins *et al.*, 1994) where the deactivation in the visual cortex decreased during the course of the learning and disappeared once the movement was learned.

TABLE 4

Each Test Condition Compared to the Control Condition

Anatomical region	BA	Coordinates (mm)			*Z* score	*P*{*Z*}	*k*	*P*{*k*, *Z*}
		x	*y*	*z*				
3D Orientation − Control								
R intraparietal sulcus or IPL	7/39	20	−70	50	5.52	<0.001	557	0.002
R inferior temporal gyrus	37	50	−54	−8	5.25	0.002	1230	0.001
R occipitotemporal junction	19/37	44	−70	−8	5.20	0.002		
R angular gyrus	39	34	−68	24	3.72	0.57		
R posterior intraparietal sulcus	19/39	38	−76	16	3.59	0.72		
L occipitotemporal junction	19/37	−42	−68	−8	4.21	0.14	270	NS 0.11
2D Orientation − Control								
R intraparietal sulcus or SPL	7	20	−64	58	4.44	0.06	149	NS 0.08
R occipitotemporal junction	19	44	−78	−4	4.06	0.23	110	NS 0.26
Size − Control								
R intraparietal sulcus	7	24	−68	42	3.64	0.66	239	NS 0.43
R inferior temporal gyrus	37	48	−56	−8	3.60	0.71	105	NS 0.47

Note. BA, Brodmann area; L, left; R, right; NS, not significant. For details see legend to Table 1.

TABLE 5

Subtraction Rest − Control and Rest − Tests

Anatomical region	BA	Coordinates (mm)			Z score	P{Z}	k	P{k, Z}
		x	y	z				
Rest − Control								
R transverse temporal gyrus	41	58	−8	2	4.16	0.17	590	0.01
R superior temporal sulcus	22	54	−12	−16	4.13	0.18		
R superior temporal gyrus	22/38	56	−2	−14	4.10	0.21		
Subcallosal ?		6	8	−14	4.15	0.18	428	0.03
R olfactive trigone?		18	6	−18	3.70	0.59		
Amygdaloid nucleus or gyrus ambiens?		−26	2	−18	4.15	0.18	473	0.02
Cortex between temporal and frontal lobes.		−40	12	−14	3.37	0.91		
		−44	18	−18	3.30	0.94		
R superior temporal gyrus	22	62	−38	0	4.12	0.19	375	0.05
R superior temporal sulcus	22/21	56	−46	10	3.96	0.31		
R superior temporal gyrus	22	60	−26	10	3.39	0.89		
Rest − Tests								
R superior temporal gyrus	22/38	56	−2	−8	5.87	<0.001	6528	<0.001
R superior temporal gyrus	22/42	60	−10	0	5.57	<0.001		
L middle frontal gyrus	10	−2	44	−4	5.39	0.001		
L superior temporal gyrus	22/38	−56	−2	−8	5.64	<0.001	2946	<0.001
L superior temporal gyrus	38	−28	6	−18	4.92	0.006		
L middle temporal gyrus	21	−56	−22	−24	4.42	0.05		
Precuneus	7	4	−54	42	4.36	0.06	579	0.013
Posterior cingular cortex	23/31	2	−54	18	4.07	0.18		

Note. BA, Brodmann area; L, left; R, right. For details see legend to Table 1.

DISCUSSION

The control condition allowed us to record cortical activity related to object vision and to eye and finger movements. Thus, the Control − Rest subtraction showed predictable rCBF increases in the whole occipital lobe, in the right hand sensorimotor cortex, in the left cerebellum, and, to a lower extent, in the SMA. The cerebellum and the SMA could have been activated by finger movements (Dupont *et al.*, 1993; Jenkins *et al.*, 1994) but also by saccadic eye movements (Petit *et al.*, 1993; Dejardin *et al.*, 1998). The role of eye movements seems unlikely, however. First, the parietal cortex, especially the IPS, was not activated during the control condition, whereas it is found to be activated during saccadic eye movements toward visual targets (Paus *et al.*, 1993; Sweeney *et al.*, 1996; Kawashima *et al.*, 1996). Moreover, neither the frontal eye fields nor the putamen nor the cerebellar vermis were activated as it could be expected from the previous descriptions of the network involved in ocular movements. Thus, our control condition appeared to be similar to a fixation condition, presumably because of the low rate of saccades performed by our subjects. Interestingly, this network was not activated either during the test conditions compared to the rest conditions.

Our results clearly show that two visual areas of the right hemisphere, namely, in the IPS and the occipitotemporal junction, are involved in discriminating spatial object attributes. These two areas were not activated in the control task even at low threshold (Control − Rest) but they were significantly activated in the three test conditions compared either with the rest or the control conditions (Tests − Control, 3D orientation − Rest, 2D orientation − Rest, Size − Rest; see Figs. 4–6). However, compared with the control condition, both foci of activation were significantly increased only during the 3D orientation condition, which suggests that their involvement is wider and more intense during the 3D orientation condition than during the other two conditions. But direct comparisons between the different test conditions do not show any rCBF differences in these areas even at low threshold.

Intraparietal Sulcus

In a previous experiment, a right IPS activation was found during both a shape matching task and an object grasping task (Faillenot *et al.*, 1997b). We suggested that IPS plays a critical role in the coding of spatial object properties such as orientation or size. The present experiment is the first to clearly demonstrate, in healthy humans, the involvement of parietal structures in the analysis of object spatial features.

This finding is in fact not surprising and is supported by neuropsychological observations. Patients with parietal lesion, especially in the right hemisphere, show

deficits related to the analysis of spatial object properties. While it is not specified whether the lesions affect the IPS (or part of it), it is plausible that it is so. Indeed lesions are often wide and the IPS runs roughly through almost the whole posterior parietal lobe. Patients with right occipitoparietal lesions show deficits on tests of line orientation and size (e.g., von Cramon and Kerkhoff, 1993). Patients with right inferior parietal lesion are no longer able to recognize familiar objects viewed under nonconventional 3D orientation whereas they have no problem in identifying objects viewed under canonical point of view (Warrington and James, 1988). Other studies described patients with specific deficit in object orientation perception (Turnbull *et al.,* 1995, 1997): in these studies familiar objects were always drawn under canonical point of view but they were sometimes presented in an unusual 2D orientation (e.g., a bus presented vertically with the wheels on the left). The patients had no problem in object identification even if the drawing was presented in an unusual orientation, although they could not report the conventional orientation of objects and showed a tendency to copy the drawings in a canonical 2D orientation when it was not (e.g., the bus was drawn horizontally with the wheels down). Thus, these patients had intact object identification but their perception of object orientation was dramatically impaired. This also suggests that object representation needed for identification integrates only the conventional views of the object and that this representation can be activated independently of the actual retinal orientation.

Thus the ensemble of these clinical observations strongly suggests that the human right IPS is involved in object orientation analysis and, to a greater extent, in the analysis of the visuospatial properties of objects. The outcome of this analysis is then available to the object identification system (distributed mainly in the occipitotemporal cortex) or to the visuomotor system (distributed mainly in the frontoparietal cortex).

One cannot exclude that the right IPS is involved in orienting attention especially for peripheral objects (Vandenberghe *et al.,* 1996, 1997). However, in our previous experiment (Faillenot *et al.,* 1997b) IPS was also found to be activated while objects were presented one by one in central vision.

Occipitotemporal Junction

The ventral activation was located in the ITG (BA 37) and in the occipital cortex posterior to the ITG (BA 19). This region is very close to the location of the middle fusiform focus (at about $x = 46$, $y = -66$, $z = -12$) described by Orban's team (e.g., Orban *et al.,* 1997; Dupont *et al.,* 1998; Cornette *et al.,* 1998; for a review see Orban *et al.,* 1998). They showed that the activity of this focus is specifically related to the comparison process (temporal or spatial comparison of a range of attributes such as motion direction or orientation). The inferior occipitotemporal junction has also been found to be activated during other matching tasks where the attributes compared were face, location (see Fig. 2 of Haxby *et al.,* 1994), and shape of unfamiliar objects (Smith *et al.,* 1995; Faillenot *et al.,* 1997a,b). Thus we suggest that the present OT focus is involved in a comparison process regardless of the attribute concerned. This does not mean that it is the only function of this region, but in our study it is probably more involved in the comparison process than in spatial analysis or perception of objects.

The neuronal specificity of the inferotemporal (IT) cortex during spatial perception has not been studied. Monkeys with TE lesions (anterior part of the IT cortex) were not impaired in learning to discriminate object orientation differing by 60° and more (Holmes and Gross, 1984). Nevertheless, it seems that the monkey TEO area (posterior part of IT cortex) shares some functional properties with the human occipitotemporal junction. Orban *et al.* (1997) and Vogels *et al.* (1997) already noted that these areas play a critical role in delayed comparison of grating orientation. Moreover, TEO neurons respond to simple and complex shapes (Kobatake and Tanaka, 1994), but their responses are modulated by physical features of the presented patterns such as size, orientation, or texture (Iwai, 1985; Tanaka *et al.,* 1991).

CONCLUSIONS

This study addressed the question of the role of parietal cortex in an object discrimination task involving spatial features. The results indicate that such task requires the contribution of both the temporal and the parietal cortices of the right hemisphere. The activated area in the intraparietal sulcus reflects spatial analysis of object while the area in the occipitotemporal junction may play a role in the comparison process involved in the task.

ACKNOWLEDGMENTS

N. Costes who programmed the stimuli, M-C. Grégoire, and F. Lavenne are gratefully acknowledged as well as the CERMEP team. This work was partially supported by a grant from the "Human Science Frontier Program." I.F. is indebted to the "Fondation pour la Recherche Médicale" for financial support.

REFERENCES

Biederman, I. 1987. Recognition by components: A theory of human image understanding. *Psychol. Rev.* **94:**115–147.

Cornette, L., Dupont, P., Rosier, A. M., Sunaert, S., Van Hecke, P., Michiels, J., Mortelmans, L., and Orban, G. A. 1998. Human brain regions involved in direction discrimination. *J. Neurophysiol.* **79:**2749–2765.

Courtney, S. M., Ungerleider, L. G., Keil, K., and Haxby, J. V. 1996. Object and spatial visual working memory activate separate neural systems in human cortex. *Cereb. Cortex* **6:**39–49.

Dejardin, S., Dubois, S., Bodart, J. M., Schiltz, C., Delinte, A., Michel, C., Roucoux, A., and Crommelinck, M. 1998. PET study of human voluntary saccadic eye movements in darkness: Effects of task repetition on the activation pattern. *Eur. J. Neurosci.* **10:**2328–2336.

Desmurget, M., Prablanc, C., Rossetti, Y., Arzi, M., Paulignan, Y., Urquizar, C., and Mignot, J.-C. 1995. Postural and synergic control of 3D movements of reaching and grasping. *J. Neurophysiol.* **74:**905–910.

Dupont, P., Orban, G. A., Vogels, R., Bormans, G., Nuyts, J., Schiepers, C., De Roo, M., and Mortelmans, L. 1993. Different perceptual tasks performed with the same visual stimulus attribute activate different regions of the human brain: A positron emission tomography study. *Proc. Nat. Acad. Sci. USA* **90:**10927–10931.

Dupont, P., Vogels, R., Vandenberghe, R., Rosier, A. M., Cornette, L., Bormans, G., Mortelmans, L., and Orban, G. A. 1998. Regions in the human brain activated by simultaneous orientation discrimination: a study with positron emission tomography. *Eur. J. Neurosci.* **10:**3689–3699.

Eacott, M. J., and Gaffan, D. 1991. The role of monkey inferior parietal cortex in visual discrimination of identity and orientation of shapes. *Behav. Brain Res.* **46:**95–98.

Faillenot, I., Sakata, H., Costes, N., Decety, J., and Jeannerod, M. 1997a. Visual working memory for shape and 3D-orientation: A PET study. *NeuroReport* **8:**859–862.

Faillenot, I., Toni, I., Decety, J., Grégoire, M.-C., and Jeannerod, M. 1997b. Visual pathways for object-oriented action and object recognition. Functional anatomy with PET. *Cereb. Cortex* **7:**77–85.

Goodale, M. A., and Milner, A. D. 1992. Separate visual pathways for perception and action. *Trends Neurosci.* **1:**20–250.

Haxby, J. V., Horwitz, B., Ungerleider, L. G., Maisog, J. M., Pietrini, P., and Grady, C. L. 1994. The functional organization of human extrastriate cortex: A PET-rCBF study of selective attention of faces and locations. *J. Neurosci.* **14:**6336–6353.

Holmes, E. J., and Gross, C. G. 1984. Effects of inferior tempora lesions on discrimination of stimuli differing in orientation. *J. Neurosci.* **4:**3063–3068.

Iwai, E. 1985. Neuropsychological basis of pattern vision in macaque monkeys. *Vision Res.* **25:**425–439.

Jenkins, I. H., Brooks, D. J., Nixon, P. D., Frackowiak, R. S. J., and Passingham, R. E. 1994. Motor sequence learning: a study with positron emission tomography. *J. Neurosci.* **14:**3775–3790.

Kawashima, R., Naitoh, E., Matsumura, M., Itoh, H., Ono, S., Satoh, K., and Gotoh, R. 1996. Topographic representation in human intraparietal sulcus of reaching and saccade. *NeuroReport* **7:**1253–1256.

Kobatake, E., and Tanaka, K. 1994. Neuronal selectivities to complex object features in the ventral visual pathway of the macaque cerebral cortex. *J. Neurophysiol.* **71:**856–867.

Kosslyn, S. M. 1994. *Image and Brain: The Resolution of the Imagery Debate.* MIT Press, Cambridge, MA.

Marr, D. 1982. *Vision: A Computational Investigation into the Human Representation and Processing of Visual Information.* Freeman, San Francisco.

Merigan, W. H., and Maunsell, J. H. R. 1993. How parallel are the primate visual pathways? *Annu. Rev. Neurosci.* **16:**369–402.

Milner, A. D., and Goodale, M. A. 1995. *The Visual Brain Inaction.* Oxford Univ. Press, Cambridge.

Ohtsuka, H., Tanaka, Y., Kusunoki, M., and Sakata, H. 1995. Neurons in monkey parietal association cortex sensitive to axis orientation. *J. Jpn. Ophtalmol. Soc.* **99:**59–67.

Orban, G. A., Dupont, P., Vogels, R., Bormans, G., and Mortelmans, L. 1997. Human brain activity related to orientation discrimination tasks. *Eur. J. Neurosci.* **9:**246–259.

Orban, G. A., and Vogels, R. 1998. The neuronalmachinery involved in successive orientation discrimination. *Prog. Neurobiol.* **55:**117–147.

Paulignan, Y., Frak, V. G., Toni, I., and Jeannerod, M. 1997. Influence of object position and size on human prehension movements. *Exp. Brain Res.* **114:**226–234.

Paus, T., Petrides, M., Evans, A. C., and Meyer, E. 1993. Role of the human anterior cingulate cortex in the control of oculomotor, manual and speech responses: A positron emission tomography study. *J. Neurophysiol.* **70:**453–469.

Petit, L., Orssaud, C., Tzourio, N., Salamon, G., Mazoyer, B. M., and Berthoz, A. 1993. PET study of voluntary saccadic eye movements in humans: Basal ganglia-thalamocortical system and cingulate cortex involvement. *J. Neurophysiol.* **69:**1009–1017.

Picard, N., and Strick, P. L. 1996. Motor areas of the medial wall: Are view of their local and functional activation. *Cereb. Cortex* **6:**342–353.

Poline, J. B., and Worsley, K. J. 1997. Combining spatial extent and peak intensity to test for activations in functional imaging. *NeuroImage* **5:**83–96.

Sakata, H., Taira, M., Kusunoki, M., and Tanaka, Y. 1997. The parietal association cortex in depth perception and visual control of hand action. *Trends Neurosci.* **20:**350–357.

Shikata, E., Tanaka, Y., Nakamura, H., Taira, M., and Sakata, H. 1996. Selectivity of the parietal visual neurons in 3D orientation of surface of stereoscopic stimuli. *NeuroReport* **7:**2389–2394.

Shulman, G. L., Corbetta, M., Buckner, R. L., Raichle, M. E., Fiez, J. A., Miezin, F. M., and Petersen, S. E. 1997. Top-down modulation of early sensory cortex. *Cereb. Cortex* **3:**193–206.

Smith, E. E., Jonides, J., Koeppe, R. A., Awh, E., Schumacher, E. H., and Minoshima, S. 1995. Spatial versus object working memory: PET investigations. *J. Cogn. Neurosci.* **7:**337–356.

Sweeney, J. A., Mintun, M. A., Kwee, S., Wiseman, M. B., Brown, D. L., Rosenberg, D. R., and Carl, J. R. 1996. Positron emission tomography study of voluntary saccadic eye movements and spatial working memory. *J. Neurophysiol.* **75:**454–468.

Taira, M., Mine, S., Georgopoulos, A. P., Murata, A., and Sakata, H. 1990. Parietal cortex neurons of the monkey related to the visual guidance of hand movement. *Exp. Brain Res.* **83:**29–36.

Talairach, J., and Tournoux, P. 1988. *Co-planar Stereotaxic Atlas of the Human Brain.* Thieme, Stuttgart.

Tanaka, K., Saito, H., Fukada, Y., and Moriya, M. 1991. Coding visual images of objects in the inferotemporal cortex of the macaque monkey. *J. Neurophysiol.* **66:**170–189.

TNO 1972. *Test for Stereoscopic Vision.* Laméris instrumenten b.v.

Turnbull, O. H., Laws, K. R., and McCarthy, R. A. 1995. Object recognition without knowledge of object orientation. *Cortex* **31:**387–395.

Turnbull, O. H., Beschin, N., and Della Sala, S. 1997. Agnosia for object orientation: Implications for theories of object recognition. *Neuropsychologia* **35:**153–163.

Ungerleider, L. G., and Mishkin, M. 1982. Two cortical visual systems. In *Analysis of Visual Behavior* (Ingle, Goodale, M. A., and Mansfield, Eds.), pp. 549–580. MIT Press, Cambridge, MA.

Vandenberghe, R., Duncan, J., Dupont, P., Ward, R., Poline, J.-B., Bormans, G., Michiels, J., Mortelmans, L., and Orban, G. A. 1997. Attention to one or two features in left or right visual field: A positron emission tomography study. *J. Neurosci.* **17:**3739–3750.

Vandenberghe, R., Dupont, P., De Bruyn, B., Bormans, G., Michiels, J., Mortelmans, L., and Orban, G. A. 1996. The influence of stimulus location on the brain activation pattern in detection and

orientation discrimination: A PET study of visual attention. *Brain* **119:**1263–1276.

Vogels, R., Saunders, R. C., and Orban, G. A. 1997. Effects of inferior temporal lesions on two types of orientation discrimination in the macaque monkey. *Eur. J. Neurosci.* **9:**229–245.

von Cramon, D., and Kerkhoff, G. 1993. On the cerebral organization of elementary visuospatial perception. In *Functional Organization of the Human Visual Cortex* (Gulyás, B., Ottoson, D., and Roland, P. E., Eds.), pp. 211–231. Pergamon Press, Oxford.

Warrington, E. K., and James, M. 1988. Visual apperceptive agnosia: A clinico-anatomical study of three cases. *Cortex* **24:**13–32.

Woods, R. P., Mazziotta, J. C., and Cherry, S. R. 1993. MRI–PET registration with automated algorithm. *J. Comput. Assist. Tomogr.* **17:**536–546.